Inverse problem in optical diffusion tomography.
IV. Nonlinear inversion formulas

Vadim A. Markel

Department of Radiology, Washington University, St. Louis, Missouri 63110

Joseph A. O'Sullivan

Department of Electrical Engineering, Washington University, St. Louis, Missouri 63130

John C. Schotland*

Departments of Electrical Engineering and Radiology, Washington University, St. Louis, Missouri 63130

We continue our study of the inverse scattering problem for diffuse light. In contrast to our earlier work, in which we considered the linear inverse problem, we now consider the nonlinear problem. We obtain a solution to this problem in the form of a functional series expansion. The first term in this expansion is the pseudo-inverse of the linearized forward-scattering operator and leads to the linear inversion formulas that we have reported previously. The higher-order terms represent nonlinear corrections to this result. We illustrate our results with computer simulations in model systems. © 2003 Optical Society of America

OCIS codes: 170.0170, 170.3010, 170.3660, 170.6960.

1. INTRODUCTION

This paper is the fourth in a series devoted to the inverse scattering problem (ISP), which arises in the context of tomographic imaging with diffuse light. In Papers I–III of the series,[1–3] we developed the scattering theory of diffusing waves in inhomogeneous media, established conditions under which the existence and the uniqueness of solutions to the linearized inverse problem are guaranteed, constructed the singular-value decomposition (SVD) of the forward-scattering operator under conditions of weak scattering, and used these results to obtain explicit inversion formulas for the case of the *linearized* ISP. The purpose of this paper is to extend these results to the *nonlinear* case.

We begin by recalling the relevant mathematical formalism from Papers I–III. We assume that the energy density $u(\mathbf{r}, t)$ of diffuse light in an inhomogeneous medium obeys the diffusion equation

$$\frac{\partial u(\mathbf{r}, t)}{\partial t} = \nabla \cdot [D(\mathbf{r})\nabla u(\mathbf{r}, t)] - \alpha(\mathbf{r})u(\mathbf{r}, t) + S(\mathbf{r}, t),$$

(1)

where $\alpha(\mathbf{r})$ and $D(\mathbf{r})$ are the position-dependent absorption and diffusion coefficients and $S(\mathbf{r}, t)$ is the power density of the source. We further assume that the source is harmonically modulated with angular frequency ω. In addition to Eq. (1), the energy density must satisfy boundary conditions on the surface of the medium (or at infinity in the case of free boundaries) of the general form

$$u + l\hat{\mathbf{n}} \cdot \nabla u = 0,$$

(2)

where l is the extrapolation length[4] and $\hat{\mathbf{n}}$ is an outward-pointing normal. Note that we obtain purely absorbing boundaries when $l = 0$ and purely reflecting boundaries when $l \to \infty$.

As shown in Papers I and II, the Green's function $G(\mathbf{r}_1, \mathbf{r}_2)$ for the frequency-domain diffusion equation obeys the integral equation

$$G(\mathbf{r}_1, \mathbf{r}_2) = G_0(\mathbf{r}_1, \mathbf{r}_2) - \int \mathrm{d}^3 r G_0(\mathbf{r}_1, \mathbf{r})V(\mathbf{r})G(\mathbf{r}, \mathbf{r}_2),$$

(3)

where G_0 is the Green's function for a homogeneous medium with absorption α_0 and diffusion constant D_0. We have also introduced the notation

$$V(\mathbf{r}) \equiv \delta\alpha(\mathbf{r}) - \nabla \cdot \delta D(\mathbf{r})\nabla,$$

(4)

where $\delta\alpha(\mathbf{r}) = \alpha(\mathbf{r}) - \alpha_0$ and $\delta D(\mathbf{r}) = D(\mathbf{r}) - D_0$. The unperturbed Green's function $G_0(\mathbf{r}, \mathbf{r}')$ obeys the boundary condition (2) and satisfies

$$(\nabla^2 - k^2)G_0(\mathbf{r}, \mathbf{r}') = -\frac{1}{D_0}\delta(\mathbf{r} - \mathbf{r}'),$$

(5)

where the diffuse wave number k is given by

$$k^2 = \frac{\alpha_0 - i\omega}{D_0}.$$

(6)

The Green's function may be directly related to the intensity measured by a point detector when the medium is illuminated by a point source. It can be shown that the change in the intensity of transmitted light (at the modulation frequency ω) due to spatial fluctuations in $\alpha(\mathbf{r})$ and $D(\mathbf{r})$ is given by the integral equation[2]

$$\phi(\mathbf{r}_1, \mathbf{r}_2) = \beta \int G_0(\mathbf{r}_1, \mathbf{r}) V(\mathbf{r}) G(\mathbf{r}, \mathbf{r}_2) \mathrm{d}^3 r. \qquad (7)$$

Here the data function $\phi(\mathbf{r}_1, \mathbf{r}_2)$ is proportional to the change in intensity relative to a reference medium with absorption α_0 and diffusion constant D_0, $\mathbf{r}_1$ and $\mathbf{r}_2$ denote the coordinates of the source and the detector, and

$$\beta = \begin{cases} 1 & \text{for free boundaries} \\ (1 + \ell^*/\ell)^2 & \text{for boundary conditions} \\ & \text{of the type (2)} \end{cases} \qquad (8)$$

with $\ell^* = 3D_0/c$.

The forward problem in diffusion tomography is defined as the problem of computing the data function ϕ from the scattering potential $\eta = (\delta\alpha, \delta D)$. More precisely, the integral equation (7) may be regarded as defining a nonlinear operator K from the Hilbert space of scattering potentials, $\mathcal{H}_1$, into the Hilbert space of scattering data, $\mathcal{H}_2$. The fact that K is nonlinear may be understood by examining the perturbation expansion for ϕ in powers of V. Using the series expansion for the Green's function G, which can be obtained by iterating the integral equation (3), and the definition of the data function (7), we obtain the required expansion:

$$\phi(\mathbf{r}_1, \mathbf{r}_2) = \beta \int \mathrm{d}^3 r G_0(\mathbf{r}_1, \mathbf{r}) V(\mathbf{r}) G_0(\mathbf{r}, \mathbf{r}_2)$$

$$- \beta \int \mathrm{d}^3 r \mathrm{d}^3 r' G_0(\mathbf{r}_1, \mathbf{r}) V(\mathbf{r}) G_0(\mathbf{r}, \mathbf{r}')$$

$$\times V(\mathbf{r}') G_0(\mathbf{r}', \mathbf{r}_2) + \cdots. \qquad (9)$$

If only the first term in the series is retained, we refer to this as the weak-scattering approximation.

The inverse problem in diffusion tomography consists in recovering η from measurements of ϕ. The standard numerical approach to this nonlinear problem is to employ a functional Newton's method.[5] This results in an iterative algorithm of the form

$$\eta_{n+1} = \eta_n + M_n^+(\phi - K[\eta_n]), \qquad n = 1, 2, ..., \quad (10)$$

where M_n^+ denotes the pseudoinverse of the functional derivative

$$M_n = \left. \frac{\delta K}{\delta \eta} \right|_{\eta = \eta_n}. \qquad (11)$$

The Newton–Kantorovich method is a variant of Newton's method in which the functional derivative M_n^+ is replaced by M_1^+ for all n. In general, this leads to an algorithm with slower convergence than Newton's method. However, the Newton–Kantorovich method is of interest, since it is possible to obtain an analytic expression for M_1^+ when $\eta_1 \equiv 0$.

In this paper we consider an alternative to the use of Newton's method. In particular, we construct a formally exact analytic solution to the nonlinear ISP. This solution, which we refer to as the inverse scattering series, has the form of a functional series expansion for η in powers of the data function ϕ. The first term in the expansion corresponds to the pseudoinverse solution to the linearized inverse problem. The higher-order terms may be

interpreted as nonlinear corrections to the SVD inversion formulas reported in Paper III. We will also show that summing the inverse scattering series to all orders is equivalent to solving the ISP by the Newton–Kantorovich method.

Series solutions to several nonlinear ISPs have been reported in the literature. These include quantum-mechanical and acoustic inverse backscattering[6,7] and nonlinear travel-time tomography.[8,9] The formal inversion of functional expansions such as the Volterra series is also well-known in nonlinear control theory. It is important to note that although the *algebraic* structure of the inverse scattering series in diffusion tomography is similar to that in quantum mechanics or acoustics, its *analytic* structure is quite different. This reflects the underlying physical difference between the short-range propagation of diffusing waves in diffusion tomography and the long-range propagation of waves in quantum mechanics or acoustics.

The remainder of this paper is organized as follows. In Section 2 we derive the inverse scattering series for diffusion tomography in its most general form, independent of geometry and the type of boundary conditions. In Section 3 we consider the inverse problem in the biplanar geometry. Finally, Section 4 describes numerical results for the nonlinear reconstruction of a spherical inhomogeneity in the biplanar geometry. Two appendixes present some mathematical properties of the inverse scattering series and the derivation of the data function for a spherical inhomogeneity in the biplanar geometry with free boundaries.

2. INVERSE PROBLEM

In this section we present the construction of the inverse scattering series for diffusion tomography. We then describe the connection to the Newton–Kantorovich method.

A. Inverse Scattering Series
The scattering series (9) can be rewritten in the form

$$\phi(\mathbf{r}_1, \mathbf{r}_2) = \int \mathrm{d}^3 r K_1^i(\mathbf{r}_1, \mathbf{r}_2; \mathbf{r}) \eta_i(\mathbf{r}) + \int \mathrm{d}^3 r \mathrm{d}^3 r'$$

$$\times K_2^{ij}(\mathbf{r}_1, \mathbf{r}_2; \mathbf{r}, \mathbf{r}') \eta_i(\mathbf{r}) \eta_j(\mathbf{r}') + \cdots, \qquad (12)$$

where

$$\eta(\mathbf{r}) = \begin{pmatrix} \eta_1(\mathbf{r}) \\ \eta_2(\mathbf{r}) \end{pmatrix} = \begin{pmatrix} \delta\alpha(\mathbf{r}) \\ \delta D(\mathbf{r}) \end{pmatrix}, \qquad (13)$$

the action of the operator V has been taken into account, and summation over repeated indices is implied with $i, j = 1, 2$. The components of the operators K_1 and K_2 are given by

$$K_1^1(\mathbf{r}_1, \mathbf{r}_2; \mathbf{r}) = \beta G_0(\mathbf{r}_1, \mathbf{r}) G_0(\mathbf{r}, \mathbf{r}_2), \qquad (14)$$

$$K_1^2(\mathbf{r}_1, \mathbf{r}_2; \mathbf{r}) = \beta \nabla_\mathbf{r} G_0(\mathbf{r}_1, \mathbf{r}) \cdot \nabla_\mathbf{r} G_0(\mathbf{r}, \mathbf{r}_2), \qquad (15)$$

$$K_2^{11}(\mathbf{r}_1, \mathbf{r}_2; \mathbf{r}, \mathbf{r}') = -\beta G_0(\mathbf{r}_1, \mathbf{r}) G_0(\mathbf{r}, \mathbf{r}') G_0(\mathbf{r}', \mathbf{r}_2),$$

$$(16)$$

$$K_2^{12}(\mathbf{r}_1,\mathbf{r}_2;\mathbf{r},\mathbf{r}')$$

$$= -\beta G_0(\mathbf{r}_1,\mathbf{r})\nabla_{\mathbf{r}'}G_0(\mathbf{r},\mathbf{r}')\cdot\nabla_{\mathbf{r}'}G_0(\mathbf{r}',\mathbf{r}_2), \quad (17)$$

$$K_2^{21}(\mathbf{r}_1,\mathbf{r}_2;\mathbf{r},\mathbf{r}')$$

$$= -\beta\nabla_{\mathbf{r}}G_0(\mathbf{r}_1,\mathbf{r})\cdot\nabla_{\mathbf{r}}G_0(\mathbf{r},\mathbf{r}')G_0(\mathbf{r}',\mathbf{r}_2), \quad (18)$$

$$K_2^{22}(\mathbf{r}_1,\mathbf{r}_2;\mathbf{r},\mathbf{r}')$$

$$= -\beta\nabla_{\mathbf{r}}G_0(\mathbf{r}_1,\mathbf{r})\cdot\nabla_{\mathbf{r}}[\nabla_{\mathbf{r}'}G_0(\mathbf{r},\mathbf{r}')\cdot\nabla_{\mathbf{r}'}G_0(\mathbf{r}',\mathbf{r}_2)]. \quad (19)$$

The components of K_n are given by

$$K_n^{i_1\cdots i_n}(\mathbf{r}_1,\mathbf{r}_2;\mathbf{R}_1,\ldots,\mathbf{R}_n)$$

$$= (-1)^{n+1}\beta\sum_{\alpha_1,\ldots,\alpha_n}\frac{\partial^{i_1-1}G_0(\mathbf{r}_1,\mathbf{R}_1)}{\partial R_{1\alpha_1}^{i_1-1}}\frac{\partial^{i_1+i_2-2}G_0(\mathbf{R}_1,\mathbf{R}_2)}{\partial R_{1\alpha_1}^{i_1-1}\partial R_{2\alpha_2}^{i_2-1}}$$

$$\times\cdots\times\frac{\partial^{i_{n-1}+i_n-2}G_0(\mathbf{R}_{n-1},\mathbf{R}_n)}{\partial R_{n-1,\alpha_{n-1}}^{i_{n-1}-1}\partial R_{n\alpha_n}^{i_n-1}}\frac{\partial^{i_n-1}G_0(\mathbf{R}_n,\mathbf{r}_2)}{\partial R_{n\alpha_n}^{i_n-1}}, \quad (20)$$

where $\alpha_1,\ldots,\alpha_n$ label Cartesian components of the vectors $\mathbf{R}_1,\ldots,\mathbf{R}_n$ and no summation should be performed over indices that are not explicitly present in the sum (i.e., for $i_k = 1$).

Observe that Eq. (12) is a functional power-series expansion, each term of which is multilinear in η. Thus we can expand ϕ in tensor powers of η:

$$\phi = K_1\eta + K_2\eta\otimes\eta + \cdots. \quad (21)$$

Here K_1 is a linear operator that maps the Hilbert space $\mathcal{H}_1$ into the Hilbert space $\mathcal{H}_2$, and K_2 may be interpreted as a tensor operator that maps $\mathcal{H}_1\otimes\mathcal{H}_1$ into $\mathcal{H}_2$. Equations (9) and (21) are analogous to the Born series in quantum scattering theory. Alternative perturbation expansions such as the Rytov series may also be considered.

If the spatial fluctuations in α and D are sufficiently small, the series (21) may be truncated after its first term. This results in an effective linearization of the forward-scattering problem with $\phi = K_1\eta$. The corresponding linear ISP has the solution $\eta = K_1^+\phi$, where K_1^+ denotes the pseudoinverse of K_1. To construct the solution to the nonlinear ISP, we act on Eq. (21) with the pseudoinverse operator K_1^+ and use the identity $K_1^+K_1 = I_{\mathcal{H}_1}$. We thus obtain

$$\eta = K_1^+\phi - K_1^+K_2\eta\otimes\eta + \cdots. \quad (22)$$

Next, by iterating this result, we find that

$$\eta = K_1^+\phi - K_1^+K_2K_1^+\otimes K_1^+\phi\otimes\phi + \cdots, \quad (23)$$

which is a functional expansion for η in tensor powers of ϕ. We will refer to Eq. (23) as the inverse scattering series for diffusion tomography.

Several comments on the above result are necessary. First, Eq. (23) provides a formally exact solution to the inverse problem in diffusion tomography. It may be viewed as a nonlinear inversion formula whose first term coincides with the pseudoinverse solution to the linearized ISP. The higher-order terms represent systematically improvable nonlinear corrections, which, in principle, can be computed to arbitrarily high order. Thus it is neces-

sary only to solve the linear ISP in order to formally solve the nonlinear ISP. Second, Eq. (23) may also be obtained by formal inversion of the functional power series (9). This results in an explicit formula for the coefficient $\mathcal{K}_n$ of the nth term in Eq. (23):

$$\mathcal{K}_n = -\left(\sum_{p=1}^{n-1}\mathcal{K}_p\sum_{i_1+\cdots+i_p=n}K_{i_1}\otimes\cdots\otimes K_{i_p}\right)\mathcal{K}_1\otimes\cdots\otimes\mathcal{K}_1,$$

$$(24)$$

where $\mathcal{K}_1 = K_1^+$ (see Appendix A). Third, it may be seen that the coefficients of all the higher-order terms in Eq. (23) have K_1^+ as a prefactor. As a result, to any finite order, the spatial resolution of images reconstructed by using the nonlinear theory can never exceed the resolution of images reconstructed by linear means alone. Fourth, the short-range propagation of diffusing waves implies that the forward-scattering problem in diffusion tomography is weakly nonlinear. This is precisely the condition under which the inverse scattering series may be expected to exhibit fast convergence. Note that a detailed analysis of the convergence of the inverse scattering series is beyond the scope of this paper. Finally, the approach to the ISP based on Eq. (23) differs from Newton-type methods. This follows from the fact that such methods require the forward problem to be solved for each iteration.

B. Relation to Newton's Method

We will now show that summing the inverse scattering series to all orders is equivalent to the Newton–Kantorovich method. To see this, we rearrange Eq. (22) as follows:

$$\eta = K_1^+(\phi - K_2\eta\otimes\eta + \cdots) \quad (25)$$

$$= K_1^+\{\phi - (K[\eta] - K_1\eta)\} \quad (26)$$

$$= \eta + K_1^+(\phi - K[\eta]) \quad (27)$$

$$\equiv T[\eta], \quad (28)$$

where in Eq. (26) we have used the functional expansion for the forward-scattering operator K. Equation (28) implies that the ISP may be reduced to the problem of finding the fixed point of the nonlinear transformation T. The fixed point may be obtained by iteration of $\eta_{n+1} = T[\eta_n]$, or, more explicitly,

$$\eta_{n+1} = \eta_n + K_1^+(\phi - K[\eta_n]), \qquad n = 1,2,\ldots. \quad (29)$$

Equation (29) coincides with the Newton–Kantorovich method if the functional derivative $M_1 = K_1$. Evidently, this condition is obeyed if the initial condition in the Newton's-method iteration (10) is chosen to be $\eta_1 \equiv 0$, that is, if the initial condition corresponds to a homogeneous medium.

3. NONLINEAR INVERSION IN THE PLANAR GEOMETRY

The inverse scattering series was developed in a form that is independent of geometry. We now specialize to

the case of the planar geometry.   Other cases including the cylindrical and spherical geometries may also be considered.

A. Inversion Formulas

In the planar geometry measurements are taken on two parallel planes.   Sources are taken to be located on the $z = 0$ plane, and detectors on the plane $z = L$.   The medium to be imaged lies between the planes in the region $0 < z < L$.   In this geometry the unperturbed Green's function is given by the plane-wave decomposition

$$G_0(\mathbf{r}, \mathbf{r}') = \int \frac{d^2q}{(2\pi)^2} g(\mathbf{q}; z, z') \exp[i\mathbf{q} \cdot (\boldsymbol{\rho} - \boldsymbol{\rho}')], \tag{30}$$

where we have used the notation $\mathbf{r} = (\boldsymbol{\rho}, z)$.   In the case of free boundaries, the function $g(\mathbf{q}; z, z')$ is given by[1]

$$g(\mathbf{q}; z, z') = \frac{\exp[-Q(\mathbf{q})|z - z'|]}{2Q(\mathbf{q})D_0}, \tag{31}$$

and in the case of boundary conditions of the type (2) by[2]

$$g(\mathbf{q}; z, z') = \frac{l}{D_0} \frac{\sinh[Q(\mathbf{q})(L - |z - z'|)] + Q(\mathbf{q})l \cosh[Q(\mathbf{q})(L - |z - z'|)]}{\sinh[Q(\mathbf{q})L] + 2Q(\mathbf{q})l \cosh[Q(\mathbf{q})L] + [Q(\mathbf{q})l]^2 \sinh[Q(\mathbf{q})L]}, \tag{32}$$

where

$$Q(\mathbf{q}) \equiv (\mathbf{q}^2 + k^2)^{1/2} \tag{33}$$

and we have assumed that either $\mathbf{r}$ or $\mathbf{r}'$ lies on one of the measurement planes.

We will find it advantageous to rewrite the inverse scattering series (23) in the form

$$\eta = \eta^{(1)} + \eta^{(2)} + \cdots, \tag{34}$$

$$\eta^{(1)} = K_1^+ \phi, \tag{35}$$

$$\eta^{(2)} = -K_1^+ K_2 \eta^{(1)} \otimes \eta^{(1)}, \tag{36}$$

where $\eta^{(1)}$ is the solution to the linearized ISP and $\eta^{(2)}$ is the first nonlinear correction.   In the planar geometry, since the measurement planes have translational symmetry, it is natural to express Eqs. (35) and (36) in the Fourier basis of two-dimensional plane waves.   In this representation Eqs. (35) and (36) become

$$\eta^{(1)}(\mathbf{r}) = \int d^2q_1 d^2q_2 K_1^+(\mathbf{r}; \mathbf{q}_1, \mathbf{q}_2) \phi(\mathbf{q}_1, \mathbf{q}_2), \tag{37}$$

$$\eta^{(2)}(\mathbf{r}) = \int d^2q_1 d^2q_2 \int d^3r' d^3r'' K_1^+(\mathbf{r}; \mathbf{q}_1, \mathbf{q}_2)$$

$$\times K_2(\mathbf{q}_1, \mathbf{q}_2; \mathbf{r}', \mathbf{r}'') \eta^{(1)}(\mathbf{r}') \eta^{(1)}(\mathbf{r}''). \tag{38}$$

Here

$$\phi(\mathbf{q}_1, \mathbf{q}_2) = \int d^2\rho_1 d^2\rho_2 \exp[i(\mathbf{q}_1 \cdot \boldsymbol{\rho}_1 + \mathbf{q}_2 \cdot \boldsymbol{\rho}_2)]$$

$$\times \phi(\boldsymbol{\rho}_1, z_1, \boldsymbol{\rho}_2, z_2), \tag{39}$$

$$K(\mathbf{q}_1, \mathbf{q}_2; \cdot) = \int d^2\rho_1 d^2\rho_2 \exp[i(\mathbf{q}_1 \cdot \boldsymbol{\rho}_1 + \mathbf{q}_2 \cdot \boldsymbol{\rho}_2)]$$

$$\times K(\boldsymbol{\rho}_1, z_1, \boldsymbol{\rho}_2, z_2; \cdot). \tag{40}$$

Note that according to Eqs. (37) and (38), once $K_1^+(\mathbf{r}; \mathbf{q}_1, \mathbf{q}_2)$ is determined, the inverse problem is solved in principle.

B. Singular-Value Decomposition of K_1^+

The SVD of the pseudoinverse operator K_1^+ is given by

$$K_1^+(\mathbf{r}; \mathbf{q}_1, \mathbf{q}_2) = \int \frac{1}{\sigma} f_\sigma(\mathbf{r}) g_\sigma^*(\mathbf{q}_1, \mathbf{q}_2) d\sigma, \tag{41}$$

where σ is the singular value associated with the singular functions f_σ and g_σ.   The singular functions are eigenfunctions with eigenvalues σ^2 of the positive self-adjoint operators $K_1^* K_1$ and $K_1 K_1^*$:

$$K_1^* K_1 f_\sigma = \sigma^2 f_\sigma, \tag{42}$$

$$K_1 K_1^* g_\sigma = \sigma^2 g_\sigma. \tag{43}$$

In addition, the singular functions are related by

$$K_1 f_\sigma = \sigma g_\sigma, \tag{44}$$

$$K_1^* g_\sigma = \sigma f_\sigma. \tag{45}$$

To proceed further, we require an explicit expression for $K_1(\mathbf{q}_1, \mathbf{q}_2; \mathbf{r})$.   This is obtained by using the definitions of G_0 from Eq. (30) and K_1 from Eqs. (14) and (15) to carry out the Fourier transformation in Eq. (40):

$$K_1(\mathbf{q}_1, \mathbf{q}_2; \mathbf{r}) = \kappa(\mathbf{q}_1, \mathbf{q}_2; z) \exp[i(\mathbf{q}_1 + \mathbf{q}_2) \cdot \boldsymbol{\rho}], \tag{46}$$

where the components of κ are given by

$$\kappa_1(\mathbf{q}_1, \mathbf{q}_2; z) = \beta g(\mathbf{q}_1; z_1, z) g(\mathbf{q}_2; z, z_2), \tag{47}$$

$$\kappa_2(\mathbf{q}_1, \mathbf{q}_2; z) = \beta \left[\frac{\partial g(\mathbf{q}_1; z_1, z)}{\partial z} \frac{\partial g(\mathbf{q}_2; z, z_2)}{\partial z} \right.$$

$$\left. - \mathbf{q}_1 \cdot \mathbf{q}_2 g(\mathbf{q}_1; z_1, z) g(\mathbf{q}_2; z, z_2) \right]. \tag{48}$$

Using Eq. (46), we find that the matrix elements of the operator $K_1 K_1^*$ are given by

$$K_1 K_1^*(\mathbf{q}_1, \mathbf{q}_2; \mathbf{q}_1', \mathbf{q}_2')$$

$$= \int d^2Q \, \delta(\mathbf{Q} - \mathbf{q}_1 - \mathbf{q}_2) \delta(\mathbf{Q} - \mathbf{q}_1' - \mathbf{q}_2')$$

$$\times M\left(\frac{1}{2}(\mathbf{q}_1 - \mathbf{q}_2), \frac{1}{2}(\mathbf{q}_1' - \mathbf{q}_2'); \mathbf{Q} \right), \tag{49}$$

where

$$M(\mathbf{P}, \mathbf{P}'; \mathbf{Q}) = (2\pi)^2 \int_0^L dz\, \kappa(\mathbf{Q}/2 + \mathbf{P}, \mathbf{Q}/2 - \mathbf{P}; z)$$

$$\times\, \kappa^*(\mathbf{Q}/2 + \mathbf{P}', \mathbf{Q}/2 - \mathbf{P}'; z). \quad (50)$$

To find the singular functions g_σ, we make the ansatz

$$g_{\mathbf{Q}\mathbf{Q}'}(\mathbf{q}_1, \mathbf{q}_2) = \int d^2P\, C_{\mathbf{Q}'}(\mathbf{P}; \mathbf{Q}) \delta(\mathbf{q}_1 - \mathbf{Q}/2 - \mathbf{P})$$

$$\times\, \delta(\mathbf{q}_2 - \mathbf{Q}/2 + \mathbf{P}), \quad (51)$$

where $\mathbf{Q}$ and $\mathbf{Q}'$ are two-dimensional wave vectors. Equation (43) now implies that

$$\int d^2P'\, M(\mathbf{P}, \mathbf{P}'; \mathbf{Q}) C_{\mathbf{Q}'}(\mathbf{P}'; \mathbf{Q}) = \sigma_{\mathbf{Q}\mathbf{Q}'}^2 C_{\mathbf{Q}'}(\mathbf{P}; \mathbf{Q}), \quad (52)$$

that is, $C_{\mathbf{Q}'}(\mathbf{P}; \mathbf{Q})$ is an eigenfunction of $M(\mathbf{P}, \mathbf{P}'; \mathbf{Q})$ labeled by $\mathbf{Q}'$ with eigenvalue $\sigma_{\mathbf{Q}\mathbf{Q}'}^2$. Note that since $M(\mathbf{Q})$ is self-adjoint, the $C_{\mathbf{Q}'}(\mathbf{P}; \mathbf{Q})$ may be taken to be orthonormal. The singular functions $f_{\mathbf{Q}\mathbf{Q}'}$ may be found from Eq. (45) by direct calculation:

$$f_{\mathbf{Q}\mathbf{Q}'}(\mathbf{r}) = \frac{1}{\sigma_{\mathbf{Q}\mathbf{Q}'}} \int d^2P \exp(-i\mathbf{Q} \cdot \boldsymbol{\rho})$$

$$\times\, \kappa^*(\mathbf{Q}/2 + \mathbf{P}, \mathbf{Q}/2 - \mathbf{P}; z) C_{\mathbf{Q}'}(\mathbf{P}; \mathbf{Q}). \quad (53)$$

It follows that the SVD of K_1^+ is given by the expression

$$K_1^+(\mathbf{r}; \mathbf{q}_1, \mathbf{q}_2) = \int d^2Q\, d^2Q' \frac{1}{\sigma_{\mathbf{Q}\mathbf{Q}'}} f_{\mathbf{Q}\mathbf{Q}'}(\mathbf{r}) g_{\mathbf{Q}\mathbf{Q}'}^*(\mathbf{q}_1, \mathbf{q}_2). \quad (54)$$

The above expression for the SVD of K_1^+ may be simplified by using the spectral decomposition

$$M^{-1}(\mathbf{P}, \mathbf{P}'; \mathbf{Q}) = \int d^2Q' \frac{1}{\sigma_{\mathbf{Q}\mathbf{Q}'}^2} C_{\mathbf{Q}'}(\mathbf{P}; \mathbf{Q}) C_{\mathbf{Q}'}^*(\mathbf{P}'; \mathbf{Q}) \quad (55)$$

and the explicit expressions for the singular functions. Equation (54) thus becomes

$$K_1^+(\mathbf{r}; \mathbf{q}_1, \mathbf{q}_2)$$

$$= \int d^2Q\, d^2P\, d^2P' \exp(-i\mathbf{Q} \cdot \boldsymbol{\rho}) M^{-1}(\mathbf{P}, \mathbf{P}'; \mathbf{Q})$$

$$\times\, \kappa^*(\mathbf{Q}/2 + \mathbf{P}, \mathbf{Q}/2 - \mathbf{P}; z) \delta(\mathbf{q}_1 - \mathbf{Q}/2 - \mathbf{P})$$

$$\times\, \delta(\mathbf{q}_2 - \mathbf{Q}/2 + \mathbf{P}). \quad (56)$$

Using this result, along with Eq. (37), we obtain $\eta^{(1)}(\mathbf{r})$, the solution to the linearized ISP:

$$\eta^{(1)}(\mathbf{r}) = \int d^2Q\, d^2P\, d^2P' \exp(-i\mathbf{Q} \cdot \boldsymbol{\rho}) M^{-1}(\mathbf{P}, \mathbf{P}'; \mathbf{Q})$$

$$\times\, \kappa^*(\mathbf{Q}/2 + \mathbf{P}, \mathbf{Q}/2 - \mathbf{P}; z)$$

$$\times\, \phi(\mathbf{Q}/2 + \mathbf{P}, \mathbf{Q}/2 - \mathbf{P}). \quad (57)$$

Note that the above inversion formula agrees with the results of Ref. 10. However, the derivation in Ref. 10 is based on a direct calculation of the pseudoinverse solution rather than a construction of the SVD of the linearized forward-scattering operator.

4. NUMERICAL RESULTS

We now illustrate the inversion formulas derived in this paper with numerical examples. We will work in the planar geometry with free boundary conditions. In addition, we assume *a priori* that there are no inhomogeneities in the diffusion coefficient ($\delta D = 0$). This allows the use of a single modulation frequency, which we set to zero. In this case the linearized inversion formula (57) can be written in the form

$$\delta\alpha^{(1)}(\mathbf{r}) = \int d^2Q\, d^2P\, d^2P' \exp(-i\mathbf{Q} \cdot \boldsymbol{\rho}) M^{-1}(\mathbf{P}, \mathbf{P}'; \mathbf{Q})$$

$$\times\, \kappa_1^*(\mathbf{Q}/2 + \mathbf{P}, \mathbf{Q}/2 - \mathbf{P}; z)$$

$$\times\, \phi(\mathbf{Q}/2 + \mathbf{P}, \mathbf{Q}/2 - \mathbf{P}), \quad (58)$$

where

$$M(\mathbf{P}, \mathbf{P}'; \mathbf{Q}) = (2\pi)^2 \int_0^L dz\, \kappa_1(\mathbf{Q}/2 + \mathbf{P}, \mathbf{Q}/2 - \mathbf{P}; z)$$

$$\times\, \kappa_1^*(\mathbf{Q}/2 + \mathbf{P}', \mathbf{Q}/2 - \mathbf{P}'; z). \quad (59)$$

In practice, this formula must be discretized. Namely, we chose the vectors $\mathbf{Q}$ to occupy a square lattice with unit step size $\Delta q = L^{-1}$ inside the circle $|\mathbf{Q}| \leq 40\Delta q$. The vectors $\mathbf{P}$, $\mathbf{P}'$ were chosen on a one-dimensional lattice coinciding with the x axis; the spacing was $\Delta p = 5\Delta q = 5L^{-1}$, and $0 \leq |\mathbf{P}| < 40L^{-1}$. Thus a total of eight different vectors $\mathbf{P}$ were used (including $\mathbf{P}=0$). Note that for numerical calculation of M^{-1}, the operator M becomes a square matrix, which can be diagonalized by the methods of linear algebra. To avoid numerical instability, the calculation of M^{-1} must be regularized. In particular, we replace $1/\sigma$ by $R(\sigma)$, where R is a suitable regularizer. The effect of regularization is to limit the contribution of small singular values to the reconstruction. The simplest way to do this is to simply cut off all σ below some cutoff σ_c. That is, we set

$$R(\sigma) = \frac{1}{\sigma} \theta(\sigma - \sigma_c), \quad (60)$$

θ denoting the usual Heaviside step function.

The forward data were calculated for a spherical absorbing inhomogeneity. The data function $\phi(\mathbf{q}_1, \mathbf{q}_2)$ is given in Appendix B. The diffuse wave numbers are given by $k_1^2 = \alpha_0/D_0$ outside the sphere and $k_2^2 = (\alpha_0 + a)/D_0$ inside the sphere. Thus, inside the sphere, we have $\delta\alpha = a = D_0(k_2^2 - k_1^2)$, and we have chosen $D_0 = 1$, $k_1 = 2\pi L^{-1}$. Reconstructions were carried out in the volume $-L \leq x, y \leq L$, $0 < z < L$, with the center of the absorbing sphere placed at the point $(0, 0, L/2)$. The sphere's radius was taken to be $R = 0.4L$, and the corresponding size parameter of the sphere was $k_1 R = 0.4$.

The results of linear reconstruction ($\delta\alpha^{(1)}$) are shown in Fig. 1. In the case $k_1 = 0.99k_2$, the weak-scattering approximation is quite accurate. As a result, the quality of reconstructed images is high, even to lowest order in
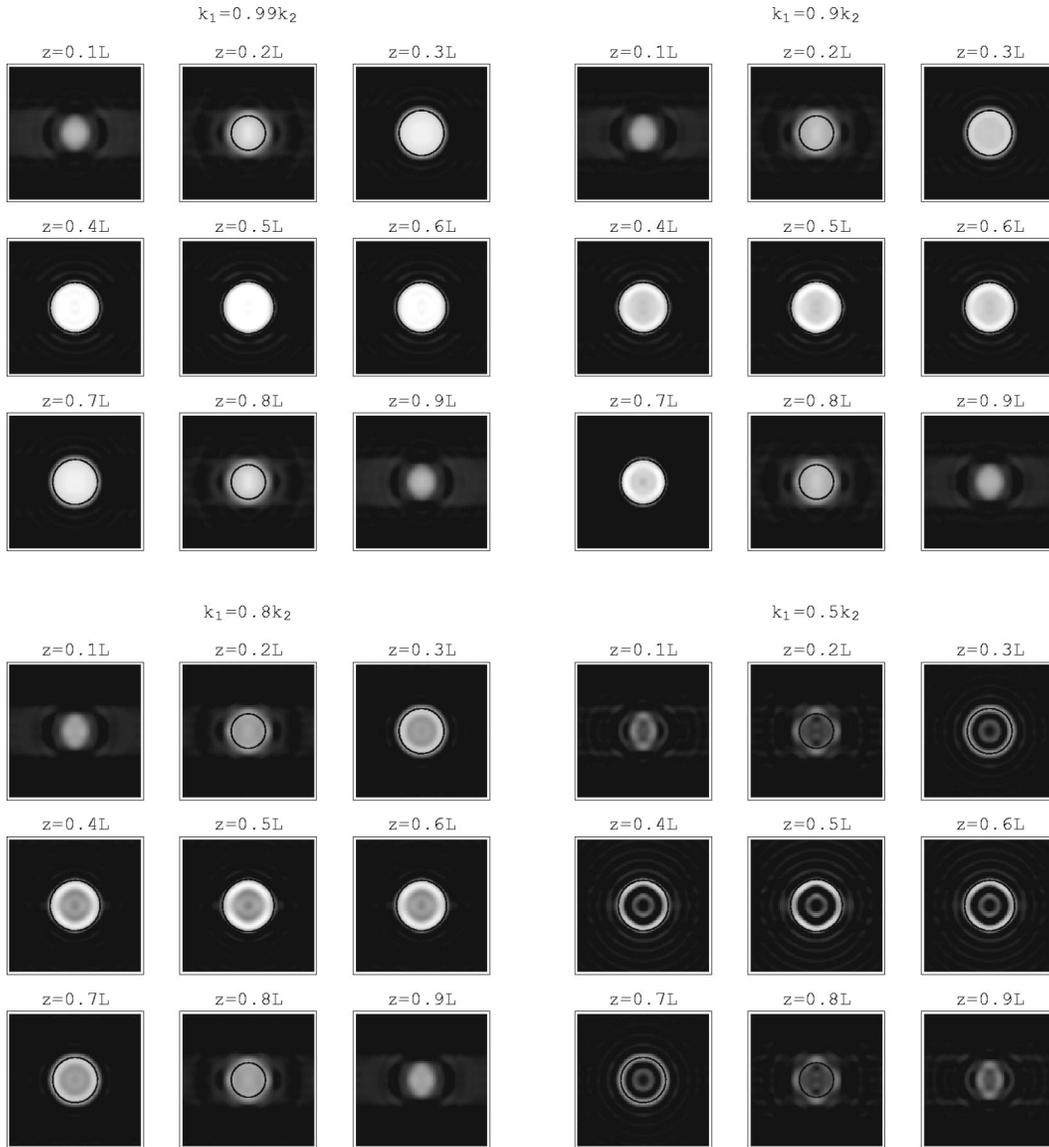
Fig. 1.   Linearized inversion with $\delta\alpha(\mathbf{r}) = \delta\alpha^{(1)}(\mathbf{r})$.   Tomographic slices are drawn at different depths z for an absorbing sphere with different values of k_2.   The solid black circles indicate the physical boundary of the absorbing sphere.   The reconstructed images are normalized by the "true" value of $\delta\alpha$, $D_0(k_2^2 - k_1^2)$.   A linear gray scale is employed; white corresponds to 1 and black to 0.

$\delta\alpha$.   As the mismatch of the absorption inside and outside the sphere becomes larger, the quality of the linearized inversion decreases.   In particular, a false dark area in the center of the sphere develops.   In the case $k_1 = 0.5k_2$ ($\delta\alpha/\alpha_0 = 3$), only a thin outer shell is reconstructed, while the inside area of the sphere is almost completely black.   This is explained by the fact that in the weak-scattering approximation the inhomogeneities are probed by the unperturbed incident field.   However, the field inside areas of greater absorption, such as the absorbing sphere in this numerical example, differs from the incident field.   In essence, the field does not penetrate into areas with very high absorption.   The linearized reconstruction "interprets" this fact as the absence of inhomogeneity.   Note that although linearized inversion is not accurate when $\delta\alpha/\alpha_0 > 1$, it still reconstructs the correct shape of an inhomogeneity.   Thus, although the internal

region of the absorbing sphere in the case $k_1 = 0.5k_2$ is not reconstructed, the overall spherical shape is reconstructed correctly.   It is expected that this is a general property of the linearized reconstruction and is not limited to spherical shapes.

We now consider the first nonlinear correction $\delta\alpha^{(2)}$, which is given by

$$\delta\alpha^{(2)}(\mathbf{r}) = -\int d^2Q\, d^2P\, d^2P'\, \exp(-i\mathbf{Q} \cdot \boldsymbol{\rho}) M^{-1}(\mathbf{P},\ \mathbf{P}';\ \mathbf{Q})$$
$$\times\ \kappa_1^*(\mathbf{Q}/2 + \mathbf{P},\ \mathbf{Q}/2 - \mathbf{P};\ z)$$
$$\times\ \phi^{(2)}(\mathbf{Q}/2 + \mathbf{P},\ \mathbf{Q}/2 - \mathbf{P}),\qquad (61)$$

where

$$\phi^{(2)}(\mathbf{q}_1, \mathbf{q}_2) = \int d^3r d^3r' K_2^{11}(\mathbf{q}_1, \mathbf{q}_2; \mathbf{r}, \mathbf{r}')$$

$$\times \; \delta\alpha^{(1)}(\mathbf{r})\delta\alpha^{(1)}(\mathbf{r}'). \qquad (62)$$

Here $K_2^{11}(\mathbf{q}_1, \mathbf{q}_2; \mathbf{r}_1, \mathbf{r}_2)$ is obtained by Fourier transformation of Eq. (16):

$$K_2^{11}(\mathbf{q}_1, \mathbf{q}_2; \mathbf{r}, \mathbf{r}')$$

$$= \frac{G_0(\mathbf{r}, \mathbf{r}')}{(2\pi D_0)^2 Q(\mathbf{q}_1)Q(\mathbf{q}_2)} \exp[i(\mathbf{q}_1 \cdot \boldsymbol{\rho} + \mathbf{q}_2 \cdot \boldsymbol{\rho}')]$$

$$\times \; \exp[-Q(\mathbf{q}_1)|z - z_1| - Q(\mathbf{q}_2)|z' - z_2|]. \quad (63)$$

The quantity $\phi^{(2)}(\mathbf{q}_1, \mathbf{q}_2)$ is calculated by numerical integration using the precomputed function $\delta\alpha^{(1)}$.

The reconstructed absorption coefficient with the first nonlinear correction ($\delta\alpha = \delta\alpha^{(1)} + \delta\alpha^{(2)}$) is shown in Fig. 2. As can be seen by comparing the panels with $k_1 = 0.8k_2$ and $k_1 = 0.9k_2$ in Figs. 1 and 2, the effect of the first nonlinear correction is to fill in the voids that are

seen in the linearized reconstruction. To illustrate this point more quantitatively, we plotted the reconstructed function $\delta\alpha$, with and without the first nonlinear correction, as a function of the x coordinate on the one-dimensional line determined by $z = $ constant, $y = 0$. The results are shown in Fig. 3. The effect of filling in the void in the center of the sphere is especially well manifested in the case $k_1 = 0.9k_2$.

As expected, the first nonlinear correction had no significant effect in the cases $k_1 = 0.99k_2$ and $k_1 = 0.5k_2$. In the first case the linearized inversion already provides accurate results, and all higher-order corrections are small. In the second case the weak-scattering approximation is strongly violated for the forward problem, and very-high-order corrections must be included to obtain convergence (provided that the series converges at all).

5. DISCUSSION

We have analyzed the nonlinear ISP for diffusing waves in inhomogeneous media. In particular, we have ob-
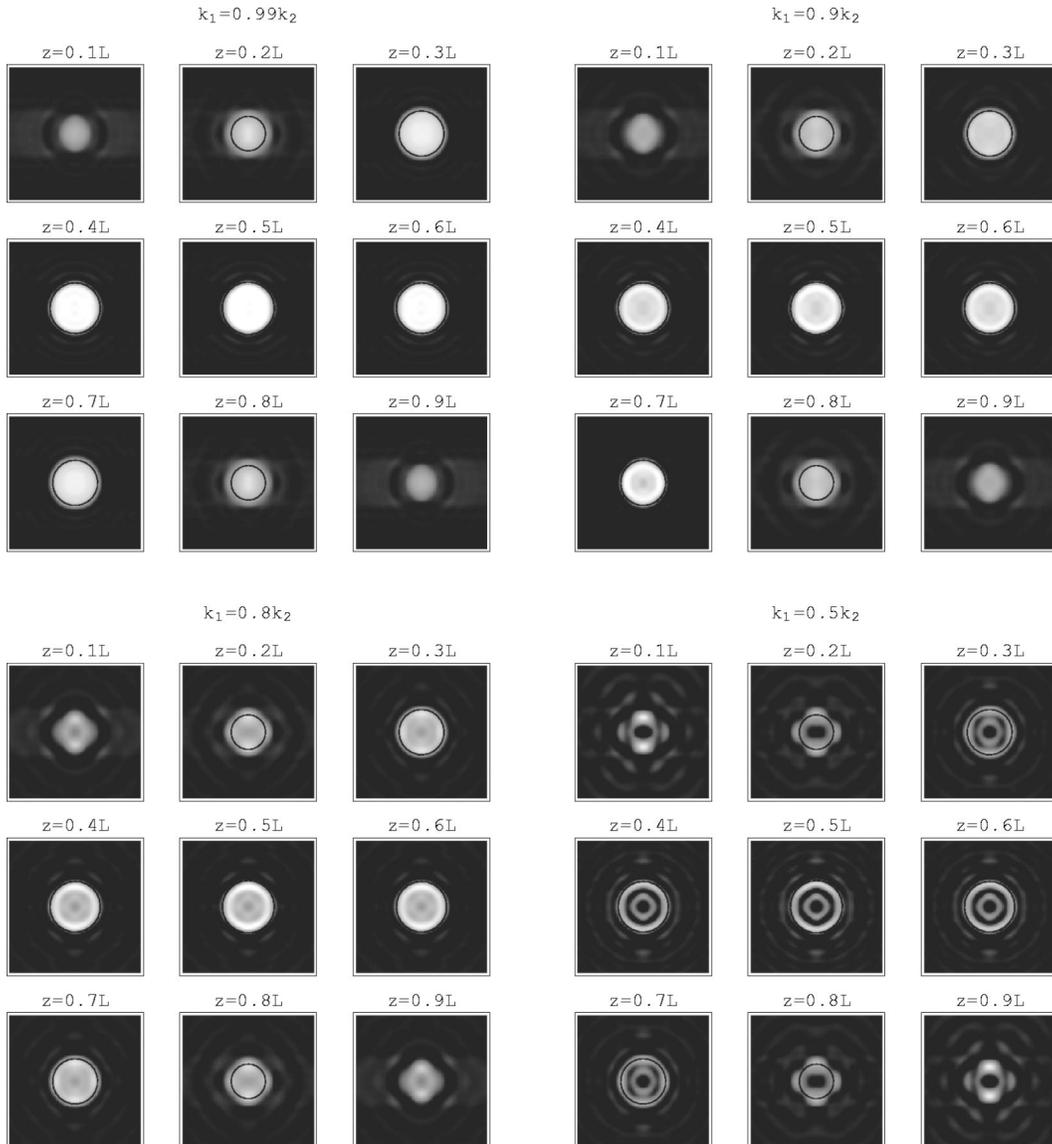
Fig. 2. First nonlinear correction $\delta\alpha(\mathbf{r}) = \delta\alpha^{(1)}(\mathbf{r}) + \delta\alpha^{(2)}(\mathbf{r})$. The same parameters as those in Fig. 1 were employed.
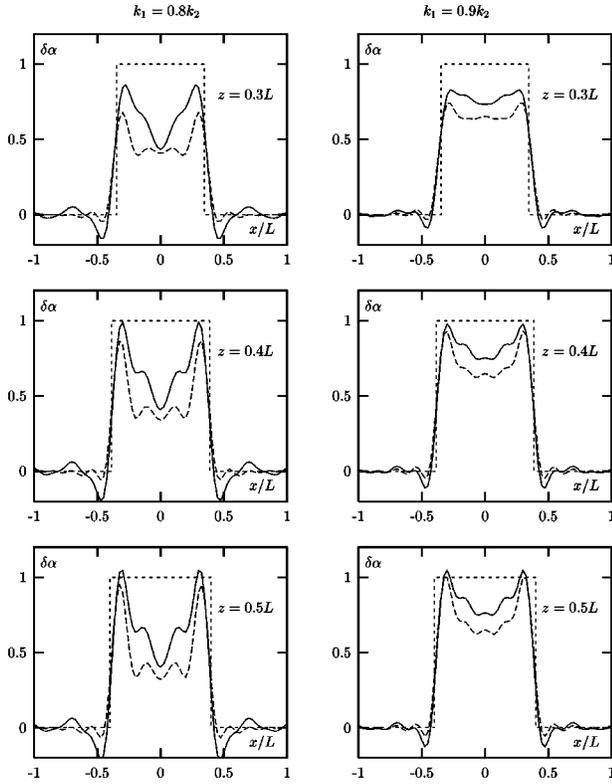
Fig. 3.   Reconstructed function $\delta\alpha(\mathbf{r})$ calculated along the line $z = $ constant (as indicated in the legend), $y = 0$, $x \in [-L, L]$. Long-dashed curves: $\delta\alpha = \delta\alpha^{(1)}$ (linearized inversion), solid curves: $\delta\alpha = \delta\alpha^{(1)} + \delta\alpha^{(2)}$ (first nonlinear correction), short-dashed curves: true profile of $\delta\alpha$.

tained a formally exact solution to this problem in the form of a functional series expansion. The first term in the expansion corresponds to the pseudoinverse solution to the linearized ISP; the higher-order terms represent nonlinear corrections. It is important to note that the methods developed in this paper are very general and apply to the ISP for any strongly damped wave such as evanescent waves or thermal waves.[11–14]

There are several issues that are important for experimental applications of the nonlinear inversion formulas. The simulations presented here consider only the case of complete data, that is, data continuously measured over the surface of the medium. However, experiments are necessarily limited to a finite amount of discrete data. Thus the effects of sampling and limited data must be considered. Results in this direction for the linear ISP have been reported in Ref. 15. In future work we intend to consider the corresponding question for the nonlinear ISP. It is also necessary to consider nonlinear corrections beyond first order. This is especially important for the reconstruction of large extended objects with high contrast. A related question is how to recover the properties of the medium with a certain spatial resolution. Here the effects of sampling and limited data are important considerations.

APPENDIX A: INVERSION OF SERIES

In this appendix we show that the inverse scattering series (23) may be obtained by formal inversion of the forward-scattering series

$$\phi = K_1\eta + K_2\eta \otimes \eta + K_3\eta \otimes \eta \otimes \eta + \cdots. \quad \text{(A1)}$$

To proceed, we assume that η may be expressed as a functional expansion in ϕ:

$$\eta = \mathcal{K}_1\phi + \mathcal{K}_2\phi \otimes \phi + \mathcal{K}_3\phi \otimes \phi \otimes \phi + \cdots, \quad \text{(A2)}$$

where $\mathcal{K}_1$ is a linear operator that maps the Hilbert space $\mathcal{H}_2$ into the Hilbert space $\mathcal{H}_1$ and $\mathcal{K}_n$ is a tensor operator that maps $\mathcal{H}_2 \otimes \cdots \otimes \mathcal{H}_2$ (n copies) into $\mathcal{H}_1$ for $n \geq 2$. To find the $\mathcal{K}$'s, we substitute the expression (A1) for ϕ into Eq. (A2) and equate terms with the same tensor power of η. We thus obtain the relations

$$\mathcal{K}_1 K_1 = I, \quad \text{(A3)}$$

$$\mathcal{K}_2 K_1 \otimes K_1 + \mathcal{K}_1 K_2 = 0, \quad \text{(A4)}$$

$$\mathcal{K}_3 K_1 \otimes K_1 \otimes K_1 + \mathcal{K}_2 K_1 \otimes K_2$$
$$+ \mathcal{K}_2 K_2 \otimes K_1 + \mathcal{K}_1 K_3 = 0, \quad \text{(A5)}$$

$$\sum_{p=1}^{n-1} \mathcal{K}_p \sum_{i_1 + \cdots + i_p = n} K_{i_1} \otimes \cdots \otimes K_{i_p}$$
$$+ \mathcal{K}_n K_1 \otimes \cdots \otimes K_1 = 0, \quad \text{(A6)}$$

which may be solved for the $\mathcal{K}$'s, with the result

$$\mathcal{K}_1 = K_1^+, \quad \text{(A7)}$$

$$\mathcal{K}_2 = -\mathcal{K}_1 K_2 \mathcal{K}_1 \otimes \mathcal{K}_1, \quad \text{(A8)}$$

$$\mathcal{K}_3 = -(\mathcal{K}_2 K_1 \otimes K_2 + \mathcal{K}_2 K_2 \otimes K_1 + \mathcal{K}_1 K_3)\mathcal{K}_1 \otimes \mathcal{K}_1 \otimes \mathcal{K}_1, \quad \text{(A9)}$$

$$\mathcal{K}_n = -\left(\sum_{p=1}^{n-1} \mathcal{K}_p \sum_{i_1 + \cdots + i_p = n} K_{i_1} \otimes \cdots \otimes K_{i_p}\right)\mathcal{K}_1 \otimes \cdots \otimes \mathcal{K}_1. \quad \text{(A10)}$$

It can be seen that the above expressions for $\mathcal{K}_1$ and $\mathcal{K}_2$ agree with Eq. (23). In addition, Eq. (A10) provides a general formula for the coefficients of the higher-order terms in Eq. (23). We note that this formula implies that the nonlinear correction of order n involves all forward operators up to order n.

APPENDIX B: DATA FUNCTION FOR A SPHERICAL INHOMOGENEITY

In this appendix we present derivation of the real-space data function for an absorbing spherical inhomogeneity in an infinite medium and calculate its Fourier transform. The real-space data function for a single spherical inhomogeneity was found earlier in Ref. 16.

Consider a spherical inclusion whose properties differ from those of the surrounding homogeneous background. We assume that $\delta D = 0$ and $\delta\alpha = a = $ constant inside a spherical region $|\mathbf{r} - \mathbf{r}_0| < R$. We will work in a reference frame whose origin coincides with the center of the sphere, $\mathbf{r}_0$. In this case the Green's function can be represented as

$$G(\mathbf{r}, \mathbf{r}') = \sum_{l=0}^{\infty} \sum_{m=-l}^{l} g_l(r, r')Y_{lm}^*(\hat{\mathbf{r}}')Y_{lm}(\hat{\mathbf{r}}), \quad \text{(B1)}$$

where the Y_{lm}'s are spherical harmonics. If both the sources and the detectors are located outside the sphere ($r, r' > R$), then

$$g_l(r, r') = \frac{2k_1}{\pi D_0}[i_l(k_1 r_<)k_l(k_1 r_>) - F_l k_l(k_1 r)k_l(k_1 r')],$$
$$(B2)$$

where $k_l(x)$ and $i_l(x)$ are the modified spherical Bessel and Hankel functions of the first kind, respectively, $r_<$ and $r_>$ are the lesser and the greater of r and r', the Mie coefficient F_l is given by

$$F_l = \frac{k_2 i_l(k_1 R)i_l'(k_2 R) - k_1 i_l(k_2 R)i_l'(k_1 R)}{k_2 i_l'(k_2 R)k_l(k_1 R) - k_1 i_l(k_2 R)k_l'(k_1 R)}, \quad (B3)$$

and k_1 and k_2 are the wave numbers outside and inside the sphere:

$$k_1^2 = \frac{\alpha_0 - i\omega}{D_0}, \qquad k_2^2 = \frac{\alpha_0 + a - i\omega}{D_0}. \quad (B4)$$

By observing that in an infinite medium the unperturbed Green's function $G_0(r, r')$ can be written as

$$G_0(\mathbf{r}, \mathbf{r}') = \frac{2k_1}{\pi D_0}\sum_{l=0}^{\infty}\sum_{m=-1}^{l} i_l(k_1 r_<)k_l(k_1 r_>)$$
$$\times Y_{lm}^*(\hat{\mathbf{r}}')Y_{lm}(\hat{\mathbf{r}}), \quad (B5)$$

we see that the first term in Eq. (B2) can be identified as the incident field, while the second term represents the scattered field. Consequently, the data function $\phi(\mathbf{r}_1, \mathbf{r}_2)$ is given by

$$\phi(\mathbf{r}_1, \mathbf{r}_2) = \frac{2k_1}{\pi D_0}\sum_{l=0}^{\infty}\sum_{m=-l}^{l} F_l k_l(k_1 r_1)k_l(k_1 r_2)$$
$$\times Y_{lm}^*(\hat{\mathbf{r}}_2)Y_{lm}(\hat{\mathbf{r}}_1). \quad (B6)$$

The above expression is valid in a reference frame whose origin is at the center of the sphere. The corresponding expression in an arbitrary reference frame is obtained by making the transformation $\mathbf{r}_{1,2} \to \mathbf{r}_{1,2} - \mathbf{r}_0$.

We now calculate the Fourier-transformed data function $\phi(\mathbf{q}_1, \mathbf{q}_2)$, which is defined by

$$\phi(\mathbf{q}_1, \mathbf{q}_2) = \int d^2\rho_1 d^2\rho_2 \exp[i(\mathbf{q}_1 \cdot \boldsymbol{\rho}_1 + \mathbf{q}_2 \cdot \boldsymbol{\rho}_2)]$$
$$\times \phi(\boldsymbol{\rho}_1, z_1, \boldsymbol{\rho}_2, z_2). \quad (B7)$$

We will show that

$$\phi(\mathbf{q}_1, \mathbf{q}_2)$$
$$= \frac{\pi^2}{2D_0 k_1 Q(\mathbf{q}_1)Q(\mathbf{q}_2)}$$
$$\times \exp[i(\mathbf{q}_2 - \mathbf{q}_1)\cdot\boldsymbol{\rho}_c - Q(\mathbf{q}_1)|z_0 - z_1| - Q(\mathbf{q}_2)|z_2 - z_0|]$$
$$\times \sum_{l=0}^{\infty}(2l+1)F_l P_l\left(\frac{\mathbf{q}_1 \cdot \mathbf{q}_2 + \gamma(z_1, z_2)Q(\mathbf{q}_1)Q(\mathbf{q}_2)}{k_1^2}\right),$$
$$(B8)$$

where the $P_l(x)$ are the Legendre polynomials and

$$\gamma(z_1, z_2) = \begin{cases} 1 & \text{if } z_1 = z_2 \\ -1 & \text{if } z_1 \neq z_2 \end{cases}. \quad (B9)$$

Note that the arguments of the Legendre polynomials in Eq. (B8) can be greater than unity; however, the Mie coefficients F_l decay with l faster than exponentially, so that the convergence of the series is guaranteed. To derive Eq. (B8), we start by expanding $\phi(\mathbf{r}_1, \mathbf{r}_2)$ in a three-dimensional Fourier integral. To this end we define $I_{lm}^1(\mathbf{p}_1)$ and $I_{lm}^2(\mathbf{p}_2)$ such that

$$k_l(k_1 r_1)Y_{lm}(\hat{\mathbf{r}}_1) = \int \frac{d^3 p_1}{(2\pi)^3}I_{lm}^1(\mathbf{p}_1)\exp(-i\mathbf{p}_1 \cdot \mathbf{r}_1), \quad (B10)$$

$$k_l(k_1 r_2)Y_{lm}^*(\hat{\mathbf{r}}_2) = \int \frac{d^3 p_2}{(2\pi)^3}I_{lm}^2(\mathbf{p}_2)\exp(-i\mathbf{p}_2 \cdot \mathbf{r}_2), \quad (B11)$$

$$I_{lm}^1(\mathbf{p}_1) = \int k_l(k_1 r)Y_{lm}(\hat{\mathbf{r}})\exp(i\mathbf{p}_1 \cdot \mathbf{r})d^3 r,$$
$$(B12)$$

$$I_{lm}^2(\mathbf{p}_2) = \int k_l(k_1 r)Y_{lm}^*(\hat{\mathbf{r}})\exp(i\mathbf{p}_2 \cdot \mathbf{r})d^3 r.$$
$$(B13)$$

The integrals (B12) and (B13) are evaluated by using the identity

$$\exp(i\mathbf{p} \cdot \mathbf{r}) = 4\pi\sum_{l=0}^{\infty}\sum_{m=-l}^{l} i^l j_l(pr)Y_{lm}^*(\hat{\mathbf{p}})Y_{lm}(\hat{\mathbf{r}}), \quad (B14)$$

where the $j_l(x)$ are spherical Bessel functions of the first kind. After expanding the exponents in Eqs. (B12) and (B13) according to Eq. (B14) and integrating over the angular variables, we obtain

$$I_{lm}^1(\mathbf{p}_1) = 4\pi i^l Y_{lm}(\hat{\mathbf{p}}_1)\int_0^{\infty} r^2 k_l(k_1 r)j_l(p_1 r)dr, \quad (B15)$$

$$I_{lm}^2(\mathbf{p}_2) = 4\pi i^l Y_{lm}^*(\hat{\mathbf{p}}_2)\int_0^{\infty} r^2 k_l(k_1 r)j_l(p_2 r)dr. \quad (B16)$$

The one-dimensional integrals are easily calculated by using the formula

$$\int_0^{\infty} x^2 k_l(ax)j_l(bx)dx = \frac{\pi}{2a}\frac{(b/a)^l}{a^2 + b^2}. \quad (B17)$$

Combining the above results, we can write the three-dimensional Fourier expansion of $\phi(\mathbf{r}_1, \mathbf{r}_2)$:

$$\phi(\mathbf{r}_1, \mathbf{r}_2)$$
$$= \frac{1}{(2\pi)^3 D_0 k_1}\sum_{lm}(-1)^l F_l$$
$$\times \int d^3 p_1 d^3 p_2 \frac{(p_1 p_2/k_1^2)^l}{(p_1^2 + k_1^2)(p_2^2 + k_1^2)}Y_{lm}(\hat{\mathbf{p}}_1)Y_{lm}^*(\hat{\mathbf{p}}_2)$$
$$\times \exp\{-i[\mathbf{p}_1 \cdot (\mathbf{r}_1 - \mathbf{r}_0) + \mathbf{p}_2 \cdot (\mathbf{r}_2 - \mathbf{r}_0)]\}, \quad (B18)$$

where we have made the shift $\mathbf{r}_{1,2} \to \mathbf{r}_{1,2} \to \mathbf{r}_0$. Thus expression (B18) is valid in an arbitrary reference frame.

Next, we decompose the three-dimensional vectors as $\mathbf{p}_1 = -\mathbf{q}_1 + t_1\hat{\mathbf{e}}_z$, $\mathbf{p}_2 = \mathbf{q}_2 + t_2\hat{\mathbf{e}}_z$, and $\mathbf{r}_0 = \boldsymbol{\rho}_0 + z_0\hat{\mathbf{e}}_z$. When we take into account that $p_{1,2}^2 = q_{1,2}^2 + t_{1,2}^2$, this immediately leads to the following expression for the two-dimensional Fourier transform of $\phi(\mathbf{r}_1, \mathbf{r}_2)$:

$$\phi(\mathbf{q}_1, \mathbf{q}_2) = \frac{2\pi \exp[-i(\mathbf{q}_1 + \mathbf{q}_2)\cdot\boldsymbol{\rho}_0]}{D_0 k_1}$$

$$\times \sum_{lm} (-1)^l F_l J_{lm}^1(\mathbf{q}_1) J_{lm}^2(\mathbf{q}_2), \quad \text{(B19)}$$

where

$$J_{lm}^1(\mathbf{q}_1) = \int_{-\infty}^{\infty} dt \, \frac{(\sqrt{q_1^2 + t^2}/k_1)^l}{q_1^2 + t^2 + k_1^2} Y_{lm}\left(\frac{-\mathbf{q}_1 + t\hat{\mathbf{e}}_z}{\sqrt{q_1^2 + t^2}}\right)$$

$$\times \exp[it(z_0 - z_1)], \quad \text{(B20)}$$

$$J_{lm}^2(\mathbf{q}_2) = \int_{-\infty}^{\infty} dt \, \frac{(\sqrt{q_2^2 + t^2}/k_1)^l}{q_2^2 + t^2 + k_1^2} Y_{lm}^*\left(\frac{\mathbf{q}_2 + t\hat{\mathbf{e}}_z}{\sqrt{q_2^2 + t^2}}\right)$$

$$\times \exp[it(z_0 - z_2)]. \quad \text{(B21)}$$

Although the integrands in Eqs. (B20) and (B21) contain square roots, they are analytic functions of t. This can be seen by examining the explicit expressions for the spherical harmonics in terms of the associated Legendre polynomials and observing that the square roots in question are raised to an even power for any l and m. Therefore Eqs. (B20) and (B21) can be evaluated by analytic continuation of the integrands into the complex plane and contour integration. The result is

$$J_{lm}^1(\mathbf{q}_1) = \frac{\pi i^l}{Q(\mathbf{q}_1)} Y_{lm}\left(\frac{-\mathbf{q}_1 + i\,\text{sgn}(z_0 - z_1)Q(\mathbf{q}_1)\hat{\mathbf{e}}_z}{ik_1}\right)$$

$$\times \exp[-Q(\mathbf{q}_1)|z_0 - z_1|], \quad \text{(B22)}$$

$$J_{lm}^2(\mathbf{q}_2) = \frac{\pi i^l}{Q(\mathbf{q}_1)} Y_{lm}^*\left(\frac{\mathbf{q}_2 + i\,\text{sgn}(z_0 - z_2)Q(\mathbf{q}_2)\hat{\mathbf{e}}_z}{ik_1}\right)$$

$$\times \exp[-Q(\mathbf{q}_2)|z_0 - z_2|]. \quad \text{(B23)}$$

Note that the spherical harmonic functions in the above expressions are analytically continued to complex angles; the arguments of Y_{lm} in Eqs. (B22) and (B23) are complex unit vectors with the property $\mathbf{a}\cdot\mathbf{a}=1$.

Finally, we use the addition theorem to perform the summation over the index m in Eq. (B19):

$$\sum_{m=-l}^{l} Y_{lm}\left(\frac{-\mathbf{q}_1 + i\,\text{sgn}(z_0 - z_1)Q(\mathbf{q}_1)\hat{\mathbf{e}}_z}{ik_1}\right)$$

$$\times Y_{lm}^*\left(\frac{\mathbf{q}_2 + i\,\text{sgn}(z_0 - z_2)Q(\mathbf{q}_2)\hat{\mathbf{e}}_z}{ik_1}\right)$$

$$= \frac{2l+1}{4\pi} P_l(\cos\theta), \quad \text{(B24)}$$

where θ is the angle between the two complex vector arguments of the spherical harmonic functions in Eq. (B24). The cosine of this angle is obviously given by

$$\cos\theta = \frac{\mathbf{q}_1\cdot\mathbf{q}_2 + \text{sgn}(z_0 - z_1)\text{sgn}(z_0 - z_2)Q(\mathbf{q}_1)Q(\mathbf{q}_2)}{k_1^2}.$$

$$\text{(B25)}$$

Taking into account that $\text{sgn}(z_0 - z_1)\text{sgn}(z_0 - z_2) = \gamma(z_1, z_2)$, we obtain the result (B8).

ACKNOWLEDGMENTS

REFERENCES

1. V. A. Markel and J. C. Schotland, "Inverse problem in optical diffusion tomography. I. Fourier–Laplace inversion formulas," J. Opt. Soc. Am. A **18**, 1336–1347 (2001).
2. V. A. Markel and J. C. Schotland, "Inverse problem in optical diffusion tomography. II. Inversion with boundary conditions," J. Opt. Soc. Am. A **19**, 558–566 (2002).
3. V. A. Markel and J. C. Schotland, "Inverse problem in optical diffusion tomography. III. Inversion formulas and singular-value decomposition," J. Opt. Soc. Am. A **20**, 890–902 (2002).
4. R. Aronson, "Boundary conditions for diffuse light," J. Opt. Soc. Am. A **12**, 2532–2539 (1995).
5. S. R. Arridge, "Optical tomography in medical imaging," Inverse Probl. **15**, R41–R93 (1999).
6. H. E. Moses, "Calculation of the scattering potential from reflection coefficients," Phys. Rev. **102**, 550–567 (1956).
7. R. T. Prosser, "Formal solutions of the inverse scattering problem," J. Math. Phys. **10**, 1819–1822 (1969).
8. R. Snieder, "A perturbative analysis of non-linear inversion," Geophys. J. Int. **101**, 545–556 (1990).
9. G. A. Tsihrintzis and A. J. Devaney, "A Volterra series approach to nonlinear travel time tomography," IEEE Trans. Geosci. Remote Sens. **38**, 1733–1742 (2000).
10. V. A. Markel and J. C. Schotland, "Inverse scattering for the diffusion equation with general boundary conditions," Phys. Rev. E **64**, R035601 (2001).
11. P. S. Carney and J. C. Schotland, "Inverse scattering for near-field microscopy," Appl. Phys. Lett. **77**, 2798–2800 (2000).
12. P. S. Carney, V. A. Markel, and J. C. Schotland, "Near-field tomography without phase retrieval," Phys. Rev. Lett. **86**, 5874–5877 (2001).
13. P. S. Carney and J. C. Schotland, "Three-dimensional total internal reflection microscopy," Opt. Lett. **26**, 1072–1074 (2001).
14. P. S. Carney and J. C. Schotland, "Determination of three-dimensional structure in photon scanning tunneling microscopy," J. Opt. A **4**, S140–S144 (2002).
15. V. A. Markel and J. C. Schotland, "Effects of sampling and limited data in optical tomography," Appl. Phys. Lett. **81**, 1180–1182 (2002).
16. D. A. Boas, M. A. O'Leary, B. Chance, and A. G. Yodh, "Scattering of diffusive photon density waves by spherical inhomogeneities within turbid media: analytic solution and applications," Proc. Natl. Acad. Sci. USA **19**, 4887–4891 (1994).